Environ Monit Assess (2018) 190: 186
https://doi.org/10.1007/s10661-018-6555-0

Performance assessment of a single-layer moisture store-and-release cover system at a mine waste rock pile in a seasonally humid region (Nova Scotia, Canada)

Christopher Power · **Murugan Ramasamy** · **Martin Mkandawire**

Received: 18 July 2017 / Accepted: 13 February 2018 / Published online: 3 March 2018

Abstract Cover systems are commonly applied to mine waste rock piles (WRPs) to control acid mine drainage (AMD). Single-layer covers utilize the moisture "store-and-release" concept to first store and then release moisture back to the atmosphere via evapotranspiration. Although more commonly used in semi-arid and arid climates, store-and-release covers remain an attractive option in humid climates due to the low cost and relative simplicity of installation. However, knowledge of their performance in these climates is limited. The objective of this study was to assess the performance of moisture store-and-release covers at full-scale WRPs located in humid climates. This cover type was installed at a WRP in Nova Scotia, Canada, alongside state-of-the-art monitoring instrumentation. Field monitoring was conducted over 5 years to assess key components such as meteorological conditions, cover material water dynamics, net percolation, surface runoff, pore-gas, environmental receptor water quality, landform stability and vegetation. Water balances indicate small reductions in water influx to the waste rock (i.e., 34 to 28% of precipitation) with the diminished AMD release also apparent by small improvements in groundwater quality (increase in pH, decrease in sulfate/metals). Surface water quality analysis and field observations of vegetative/aquatic life demonstrate significant improvements in the surface water receptor. The WRP landform is stable and the vegetative cover is thriving. This study has shown that while a simple store-and-release cover may not be a highly effective barrier to water infiltration in humid climates, it can be used to (i) eliminate contaminated surface water runoff, (ii) minimize AMD impacts to surface water receptor(s), (iii) maintain a stable landform, and (iv) provide a sustainable vegetative canopy.

Keywords Acid mine drainage · Contaminant remediation · Hydrogeochemistry · Environmental monitoring · Water balance · Landform stability

C. Power (✉) · M. Ramasamy · M. Mkandawire
Verschuren Centre for Sustainability in Energy and the Environment, Cape Breton University, Sydney, Nova Scotia, Canada
e-mail: chris_power@cbu.ca

M. Ramasamy
e-mail: murugan_ramasamy@cbu.ca

M. Mkandawire
e-mail: martin_mkandawire@cbu.ca

Introduction

Mine waste rock piles (WRPs) are anthropogenically created landforms in active and former mining areas that pose a significant environmental hazard. WRPs can contain significant quantities of sulfidic minerals and their interaction with oxygen and water can cause a complex sequence of oxidation-reduction reactions that produces a leachate characterized by low pH and high acidity. This acidic leachate can then further dissolve other minerals in the waste rock and become enriched with sulfate, iron, manganese, and other toxic heavy metals, producing acid mine drainage (AMD) (e.g., Blowes et al. 2014; Amos et al. 2015).

AMD from WRPs can cause severe environmental impacts, particularly on soil, water resources, and aquatic communities (e.g., Akcil and Koldas 2006; Sracek et al. 2010). Cover systems are commonly applied over WRPs to prevent and/or control AMD by isolating the reactive waste and limiting the influx of meteoric water and atmospheric oxygen (e.g., Johnson and Hallberg 2005; Kefeni et al. 2017). In addition to controlling contaminant releases, cover systems can provide physical and chemical stabilization of the waste and a growth medium for establishing sustainable vegetation.

Cover system design depends on several factors, including site conditions (i.e., climate, hydrogeology, waste rock geochemistry), installation complexity and cost, material availability, and required performance criteria (INAP 2014; Power et al. 2017). As a result, cover systems employed worldwide have been simple or complex, ranging from a single-layer of earthen material to multiple layers of different material types, including native soils, oxygen-consuming materials, and/or geosynthetic materials (e.g., Kim and Benson 2004; MEND 2004; Salinas Villafane et al. 2012).

A single-layer moisture store-and-release cover system is the most straightforward option to implement at WRP sites. A single-layer of earthen material acts to limit water influx by storing water within the material during high precipitation (PPT) periods and subsequently releasing it back to the atmosphere via evapotranspiration during dry periods (e.g., O'Kane and Ayres 2012; Power et al. 2018). This cover type is most commonly used in semi-arid and arid climates, where potential evaporation (PE) exceeds PPT (e.g., Scanlon et al. 2005; Bonstrom et al. 2012).

In humid regions, water storage can be overwhelmed in a single soil layer, so an underlying "barrier" layer, such as low hydraulic conductivity soils, geosynthetic clay liners (GCLs), or geomembrane liners, is added to promote "water-shedding" (e.g., Benson et al. 2007; Power et al. 2017). However, the performance of these multilayer systems can still be affected over time in seasonally humid regions: low hydraulic conductivity soil layers are typically unable to maintain a high degree of saturation throughout the year (e.g., Ayres et al. 2003), while compacted clay liners and GCLs can be significantly affected by desiccation and freeze-thaw cycling (e.g., Albright et al. 2006; Meer and Benson 2007).

The large seasonal temperature variance prevalent in humid climates, with warm-to-hot summers and cold-to-severely cold winters, poses a significant challenge to cover performance regardless of the number or complexity of layers. Therefore, while single-layer covers may not be as effective as multilayer covers in limiting water infiltration to the waste rock (e.g., Adu-Wusu and Yanful 2006), they can still be an attractive closure option to meet other performance criteria (e.g., stable landform, sustainable vegetation canopy). Single-layer covers are the least complex and most inexpensive system to install and maintain at WRPs, particularly when the soil material can be sourced locally, while material for multilayer systems usually needs to imported and can be extremely expensive. For example, a single soil layer can cost \$12/m^2 to install while the addition of a barrier layer can increase the cost to \$33/m^2 (Power et al. 2017).

A comprehensive assessment of the spatial and temporal performance of single-layer cover systems applied in seasonally humid regions would help to better understand the interactions between climatic conditions, cover material water dynamics and environmental receptors, and highlight its effectiveness related to typical performance criteria. Such an assessment requires a range of field instrumentation to measure key parameters such as PPT, actual evapotranspiration (AET), cover material moisture storage, pore-gas concentrations, soil temperature, surface runoff (R), and water quality (e.g., O'Kane et al. 1998). This level of assessment on single-layer covers in humid climates has been limited to a handful of studies at only small test WRPs (e.g., Ayres et al. 2003; Adu-Wusu et al. 2007). Very few, if any, studies have been conducted with extensive instrumentation at full-scale, in-service WRPs.

The objective of this study was to comprehensively assess the field performance of a moisture store-and-release cover system employed at WRPs in seasonally humid regions. The study site is located in Nova Scotia, Canada, and contains a full-scale WRP reclaimed with a single-layer store-and-release cover. A comprehensive 5-year field monitoring program was subsequently conducted with state-of-the-art field instrumentation to continuously monitor a number of key components and interactions including meteorological conditions, cover material moisture dynamics, net percolation into the waste rock, pore-gas, surface runoff, cover vegetation and erosion, and AMD impacts to the receiving environment.

Material and methods

Study site

The Sydney Coalfield in Nova Scotia, Canada is the oldest mined coal field in North America, with underground mining occurring from the early 1700s to the early 2000s. The former Lingan Mine Colliery is located approximately 15 km from Sydney, Nova Scotia. The colliery was operational between 1970 and 1992, facilitating the extraction of 28 million tonnes of coal from the Lingan Harbour Seam. During operation, surplus coal fines and mine waste rock from both the Lingan colliery and the adjacent former Phalen Colliery were deposited into a WRP (Power et al. 2018).

After the closure of operations in 1992, the Lingan WRP contained 250,000 m^3 of waste rock, with an additional 130,000 m^3 of waste rock relocated from the Phalen Colliery and placed on top of the pile in 2008. The consolidated WRP contains 380,000 m^3 (646,000 t) of waste rock, covering an area of 82,000 m^2. It is approximately 15 m high, with slopes ranging between 1 and 10% on top of the pile and 4 and 20% on the sides. A plan view of the Lingan WRP and surrounding area is shown in Fig. 1. The site lies in a humid continental region.

The WRP is underlain by native till, with a layer thickness ranging from 0.5 to 5.2 m, and bedrock, as illustrated by the vertical cross section in Fig. 1 (inset). The key geotechnical properties—hydraulic conductivity, porosity, and particle size distribution—of the waste rock, till, and bedrock units are presented in Table 1.

AMD contamination

Acid-base accounting (ABA) testing on extracted waste rock samples confirmed that the WRP was acid generating. Furthermore, AMD was observed in the environmental receptors: (i) groundwater flowing

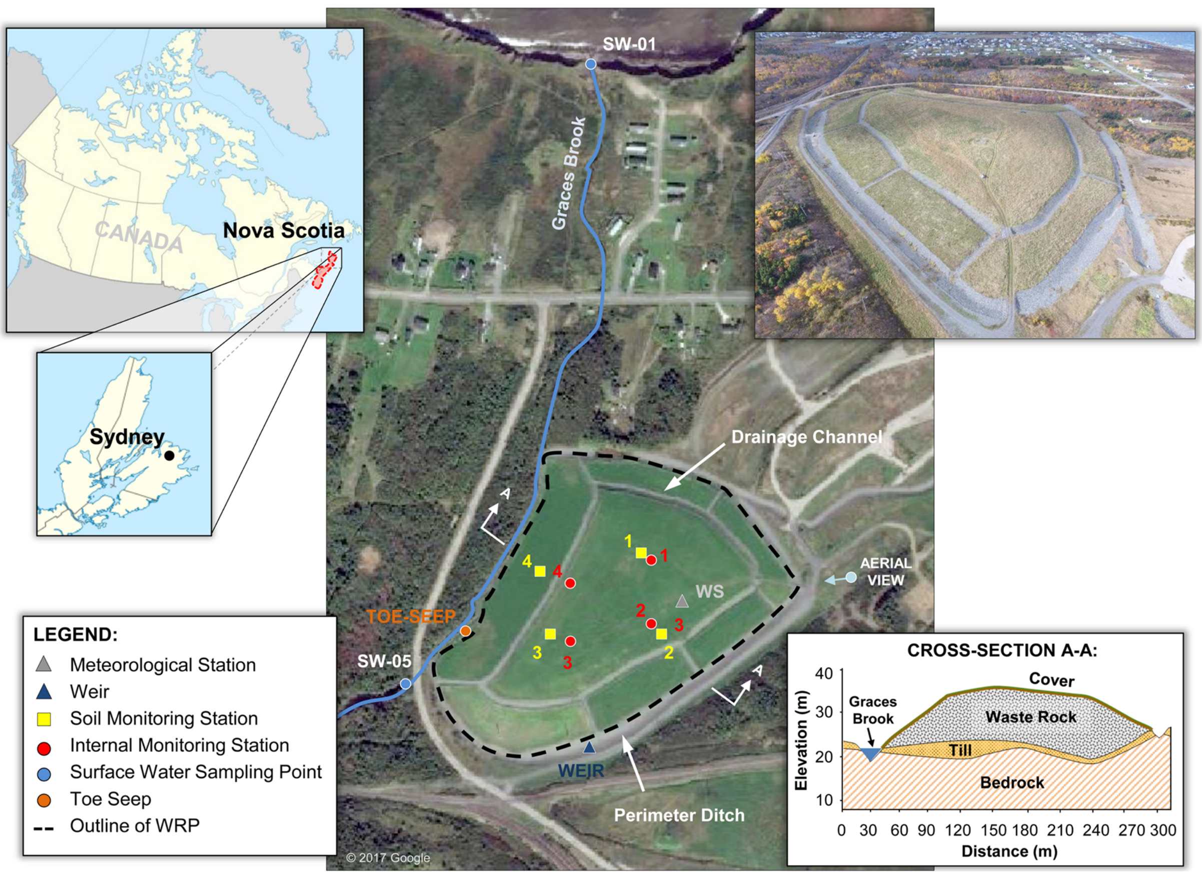

Fig. 1 Plan view (main) of the Lingan WRP and surrounding area, including key features. An aerial photograph of the pile is also shown (inset—top) along with a geological cross-section through the WRP (inset—bottom)

Table 1 Geotechnical properties of each hydrostratigraphic unit at the Lingan WRP site

Unit	Hydraulic conductivity (m/s)	Porosity (−)	Particle size distribution (%)[b]
Cover material	2.72×10^{-7} to 5.38×10^{-5} [a]	0.40	36/43/21
Waste rock	2.78×10^{-6} to 9.08×10^{-5}	0.35	38/44/18
Till	5.09×10^{-7} to 1.69×10^{-5}	0.25	28/40/32
Bedrock	4.37×10^{-7} to 1.24×10^{-5}	0.12	–

[a] In situ saturated hydraulic conductivity measured with a Guelph Permeameter

[b] Particle size distribution percentages are listed as "gravel"/"sand"/"silt/clay"

beneath the WRP and (ii) the stream (Graces Brook) flowing adjacent to the western slope of the pile (see Fig. 1). Historically, AMD loading to groundwater occurred through downward pore-water seepage at the base of the pile (i.e., basal seepage), while surface water runoff, groundwater seepage at an isolated location at the toe of the pile (i.e., toe seep indicated in Fig. 1), and groundwater discharge all contributed to AMD loading to Graces Brook.

Cover system

In 2011, a moisture store-and-release cover system was installed over the Lingan WRP to mitigate impacts to the receiving environment. The cover system consists of a 0.5-m-thick growth medium of till material sourced from local borrow areas. The cover system was then hydro-seeded to promote the establishment of sustainable vegetation. Drainage ditches were installed around the perimeter of both the plateau and base of the WRP to help manage and divert surface runoff from the pile, and toe seepage water, into Graces Brook and prevent soil cover erosion. Toe protection was also installed at the base of the WRP for long-term protection and stability. Figure 2 presents a profile of the cover system.

The physical characteristics of the cover material are similar to that of the waste rock (see Table 1). Given these similarities, and also the humid continental climate in the region, it was expected that the primary mechanism for mitigating impacts to the receiving environment would

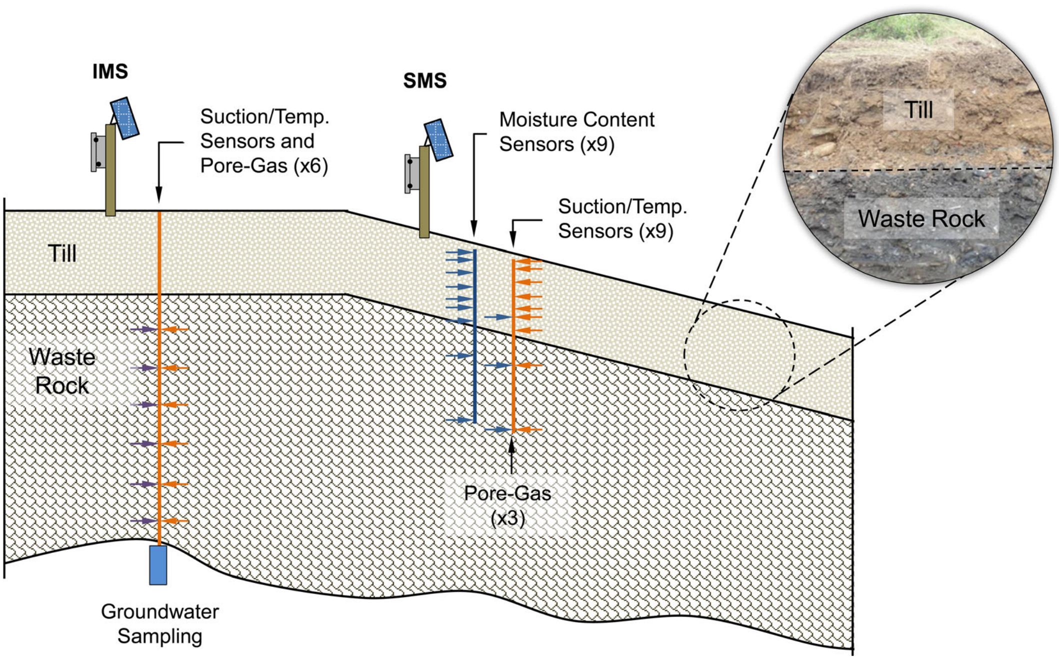

Fig. 2 Cross-section of the WRP showing the profile of the cover system, along with a Soil Monitoring Station (SMS) and Internal Monitoring Station (IMS) and associated monitoring parameters

be through the removal of contaminated surface water runoff from the pile. This would minimize AMD impacts on Graces Brook in the short term and facilitate its recovery in the long term.

Field monitoring program

Various monitoring instrumentation were installed at the WRP in February 2011 to facilitate evaluation of cover system performance over time under site-specific climatic conditions. Figure 3 presents photographs of some of the installed field instruments.

Meteorological conditions

A meteorological station measured rainfall, air temperature, relative humidity, wind speed and direction, barometric pressure, net radiation, and snowpack depth at the pile. A secondary meteorological station that measured net radiation and snowpack depth is located on the pile slope at Soil Monitoring Station 4 (SMS-4). Meteorological parameters were measured every 60 s, with hourly and daily averages stored by robust Campbell Scientific data acquisition systems (DASs).

Snow surveys were conducted at designated cover locations throughout each winter to determine the depth and density of the snowpack on the cover. Snowpack density was estimated from snow core samples taken during the snow surveys, while manual snow depth measurements were used to verify the automatic snow depth measurements recorded hourly by the meteorological station.

Surface runoff

A 60° V-notch weir monitored runoff flow rates in the perimeter ditch at the southern WRP location indicated in Fig. 1. This location was selected to ensure that weir measurements are indicative of runoff from the WRP surface and minimize capturing runoff from the surrounding natural landscape. A sonic ranger and water conductivity and temperature probe were used to obtain hourly stage, ambient temperature, discharge water temperature, and electrical conductivity (EC) measurements.

Cover material and shallow waste rock

AET was estimated using an Eddy Covariance system. The system was installed at the Lingan

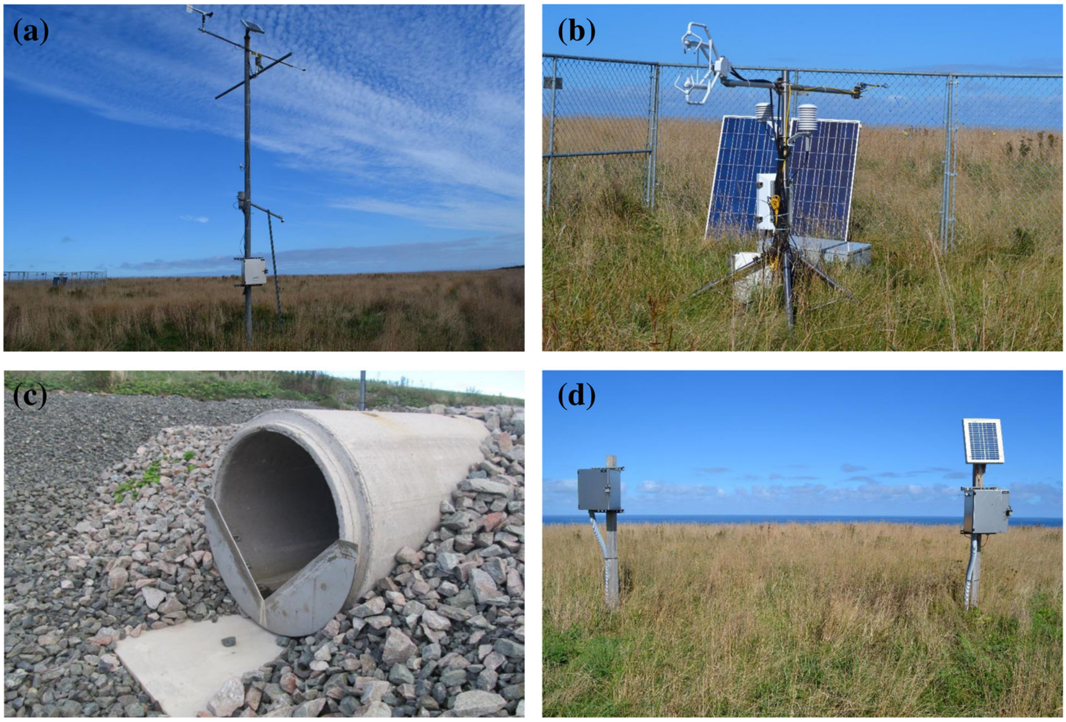

Fig. 3 Photographs from the Lingan WRP showing the **a** meteorological station, **b** Eddy Covariance system, **c** weir, and **d** Soil Monitoring Station 1 (right) and Internal Monitoring Station 1 (left)

WRP in 2015 to obtain a direct site measurement of AET. It was also installed at the nearby Victoria Junction WRP in 2013 and 2014, and at the Scotchtown Summit WRP in 2016. AET/PE ratios developed at these other sites were applied to PE measurements from the Lingan WRP to obtain a site-specific AET. The Eddy Covariance system was not in operation during the winter, and a correlation developed between the measured AET/PE ratio and soil moisture conditions was used.

Four SMSs were installed across the WRP to continuously monitor moisture and temperature conditions within the cover and shallow waste rock material. SMS-1 to SMS-3 were installed on the plateau of the pile, while SMS-4 was installed on the slope where cover system performance should be different as a result of higher runoff and differences in net radiation, snowpack formation, evapotranspiration, and vegetation development. At all stations, thermal conductivity sensors measured in situ matric suction (negative pore-water pressure), while time domain reflectometry (TDR) sensors measured in situ volumetric moisture content. These sensors were installed along single depth profiles at each station, with sensor depths of 0.05, 0.10, 0.20, 0.30, 0.40, 0.48, 0.55, 1.20, and 1.80 m, as illustrated in Fig. 2. Each parameter was automatically recorded every 3 h by DAS.

Three sampling ports were installed at each SMS to measure oxygen (O_2) and carbon dioxide (CO_2) concentrations. The upper, middle, and lower sampling port depths correspond to the growth medium (0.48 m), just below the cover–waste rock interface (0.55 m), and approximately 0.70 m into the waste rock (1.20 m). A portable gas analyzer was connected to the sampling line for each port to manually measure pore-gas concentrations every month.

Internal waste rock pile

Four internal monitoring systems (IMSs) were installed in the WRP through the entire depth of the waste rock and completed in the shallow bedrock (depths ranging from 13.7 to 19.7 m). Each IMS consists of a well that is instrumented with six temperature probes and continuous multi-channel tubing (CMT). The CMT provided six sampling depths, ranging from 1.4 to 14.9 m, with pore-gas pressure automatically monitored every 3 h at two depths and pore-gas concentrations manually measured at the remaining depths (see Fig. 2).

Waste rock samples were collected during drilling of each IMS in February 2011 and stored for subsequent analysis. Waste rock samples were also collected during monitoring well drilling and test pit excavations conducted across the WRP in 2008.

Environmental receptors

Each IMS contains a central channel that extends to its base within the shallow bedrock. Groundwater levels and groundwater samples (for chemical analysis) were regularly collected through this channel between June 2012 and December 2016. In 2008, numerous groundwater monitoring wells had been installed across the site to measure groundwater levels and groundwater chemistry (September 2008 and December 2008). Although these wells were decommissioned during cover system installation, the available data provides site conditions prior to remediation (i.e. pre-cover).

Surface water flow rates and chemistry were monitored at two sampling locations along Graces Brook between June 2008 and December 2016: upstream (SW-05) and downstream (SW-01) of the WRP (Fig. 1). Table 2 presents a summary of the various elements employed in the field monitoring program at the Lingan WRP, along with the associated monitoring parameters and time periods.

Landform stability and vegetation

Site inspections, including erosion surveys, vegetation surveys, and aerial inspections, were conducted at the site annually to monitor the stability of the landform and evolution of the vegetative cover.

Site conceptual model

Atmosphere

PPT is the product of rainfall and snow water equivalent (SWE). While rainfall was directly measured by the meteorological station, SWE, which is the measurement of how much water is present in a snowpack, was indirectly determined from snowpack density and depth.

Cover material

In addition to PPT, the amount and redistribution of PE are the main drivers of cover system water dynamics. Sufficient information was available to estimate PE [mm/day] from the widely used Penman (1948) method:

$$PE = \frac{(m \cdot R_n + E_a \cdot \gamma)}{(m + \gamma)} \quad (1)$$

where m is the slope of the saturation vapor pressure curve ($\delta e^o/\delta T$, where e^o is the saturated vapor pressure [Pa] and T is the air temperature [K]), R_n is the net radiation [MJ/m^2/day], E_a is the vapor transport of flux [mm/day], and γ is the psychrometric constant [Pa/K].

Numerical modeling indicated that the contributing WRP surface area for runoff to the weir was 26,000 m^2. The water volume discharging from the weir was calculated from the stage height measurements and weir geometry. This discharge volume was then integrated with the contributing surface area to estimate the volume of runoff from the WRP.

A thorough understanding of the cover system moisture dynamics on a spatial and temporal basis is essential to assess the performance of the moisture store-and-release cover. As SMS-1 to SMS-3 were located on the plateau and SMS-4 was located on a side slope, spatial differences in cover system conditions could be monitored. The volumetric moisture contents measured at the six depths within the growth medium, ranging from 0.05 to 0.48 m, were compiled to determine the total volume of water in the cover material.

Annual water balances between 2012 and 2016 were also developed to better understand cover system dynamics (e.g., Barber et al. 2015) and consisted of the following components:

$$PPT = R + AET + \Delta WS + \Delta SS + NP \quad (2)$$

where ΔWS is the change in water storage, ΔSS is the change in snow storage, and NP is net percolation. NP is estimated as the residual of Eq. (2) and indicates the water flux through the cover and into the waste rock.

Oxygen flux through the cover to the underlying waste material can occur through molecular diffusion, barometric pumping, and dissolved O_2 within percolating water. Diffusive O_2 flux, which is driven by the concentration gradient across the cover-waste rock interface, was estimated by Fick's Law which has been widely used to evaluate diffusive flux through various covers (e.g., Aubertin et al. 2000):

$$J_{\text{diff}} = -D^{\Delta C}/_{\Delta x} \quad (3)$$

where D is the diffusivity coefficient [m^2/s], ΔC is the change in O_2 concentration [mol/m^3], and Δx is the distance across the cover/waste interface [m]. The diffusivity coefficient is determined by (e.g., Kim and Benson 2004):

$$D = \tau D_a [1 - S_w]^a + \tau S_w D_w / K_h \quad (4)$$

where D_a and D_w are the free diffusion coefficients of O_2 in air (2×10^{-5} m^2/s) and water (1.8×10^{-9} m^2/s), respectively, τ is a tortuosity factor (~0.3), a is an empirical coefficient (~3.3), S_w is the measured water saturation in the cover, and K_h is Henry's constant for O_2. Equation (4) provided a bulk diffusion coefficient corresponding to parallel diffusion in the gas and liquid phases, with the left-hand term ($\tau D_a[1 - S_w]^a$) corresponding to the gas phase. The diffusion coefficient was then integrated with the measured O_2 gradient between 0.48 and 0.55 m.

Advective O_2 flux can occur through barometric pumping, which is dependent on the magnitude and duration of changes in atmospheric pressure and air conductivity in the cover material. Advective flux was found to be negligible, as although barometric pumping is causing O_2 to breath in and out of the cover, the maximum penetration depth does not exceed the cover thickness (e.g., maximum O_2 depth in 2014 was equal 0.33 m). Dissolved O_2 flux was determined by combining dissolved O_2 concentration with NP.

Waste rock

Waste rock acidity exists in two forms: stored acidity or potential acidity. Stored acidity is existing acidity that is readily available for transport to the receiving environment, while potential acidity first requires oxidation of the sulfide minerals to generate "additional" stored acidity.

ABA tests are well established and widely accepted to characterize waste rock acidity (e.g., Parbhakar-Fox and Lottermoser 2015; Yucel and Baba 2016). ABA tests were performed on eight stored waste rock samples from the IMSs: one shallow and one deep sample were used from each IMS. In 2008, ABA testing was performed on 26 waste rock samples collected across the site.

The total O_2 flux can be converted to an acidity load on the basis of H_2SO_4 equivalent (mol/m^2/year). The overall summary reaction of pyrite weathering to form AMD is shown in Eq. (5), where oxidation of 1 mol of pyrite (FeS_2) generates 2 mol of sulfuric acid (H_2SO_4) per 3.75 mol of O_2 present (Nordstrom et al. 2015):

$$FeS_2 + {}^{15}/_{4}O_2 + {}^{7}/_{2}H_2O \rightarrow Fe(OH)_3 + 2H_2SO_4 \quad (5)$$

Environmental receptors

The evolution of AMD and groundwater quality underlying the pile was determined from samples collected periodically at each IMS. AMD is generally characterized by sulfate, pH, alkalinity, and dissolved concentrations of iron, aluminum, and manganese. An estimate of "pre-cover" groundwater quality was obtained from representative historical wells that were previously active and screened at similar locations and depths to the IMSs. As indicated in Fig. 1, MW-11 was located at the center of the pile plateau between all four IMSs and provides groundwater quality at the center of the pile. MW-02 was located on the western slope and provides "downgradient" groundwater quality. Based on groundwater flow, it was most representative to compare IMS-1 and IMS-2 to MW-11 and IMS-3 and IMS-4 to MW-02.

Surface water measured upstream at SW-05 provides the background water quality prior to interaction with AMD from the WRP, while surface water measured downstream at SW-01 provides the water quality following contamination with AMD.

The majority of acidity in mine water arises from free protons (manifested in low pH) and the mineral acidity arising from dissolved iron, aluminum, and manganese (Watzlaf et al. 2004). The acidity of a mine water sample can be calculated from its pH and the sum of the milliequivalents of the dissolved acidic metals. In many AMD studies, the acidity is calculated as follows (e.g., Kirby and Cravotta 2005; Park et al. 2015):

$$\text{Acidity}_{\text{calc}} = 50\cdot\{2\cdot[\text{Fe}]/56 + 3\cdot[\text{Al}]/27 + 2\cdot[\text{Mn}]/55 + 1000\cdot10^{(-\text{pH})}\}, \quad (6)$$

where iron (Fe), aluminum (Al), and manganese (Mn) are dissolved concentrations [mg/L], and 50 is the equivalent weight of $CaCO_3$, which converts the acidity in milliequivalents per liter into milligrams per liter of $CaCO_3$ equivalent. Numerous studies have demonstrated that the acidity calculated from Eq. (6) is in good agreement with measured acidities over a broad range of pH values (e.g., Watzlaf et al. 2004; Kirby and Cravotta 2005).

Table 2 Summary of the Lingan WRP site monitoring elements and parameters

Monitoring element	Number	Parameters	Material	Monitoring period
Meteorological station	1	Rainfall, air temperature, relative humidity, wind speed and direction, barometric pressure, snowpack depth, net radiation	Atmosphere and cover	January 12–December 16
Weir	1	Surface runoff from WRP	Cover	January 12–December 16
Soil monitoring station	4	In situ temperature, matric suction, volumetric moisture content, O_2/CO_2 pore-gas concentrations	Cover and waste rock (shallow)	January 12–December 16
Internal monitoring station	4	Pore-gas pressure, temperature, O_2/CO_2 pore-gas concentrations, groundwater level, water chemistry[a]	Waste rock (deep) and groundwater	January 12–December 16
Groundwater monitoring well[b]	8	Groundwater level, water chemistry[a]	Groundwater	September 08–December 08
Surface water sampling point	2	Surface water flow rate, water chemistry[a]	Surface water	January 08–December 16

[a] Includes pH, alkalinity, EC, turbidity, sulfate, total/dissolved metals, acidity, total dissolved solids (TDS), and total suspended solids (TSS)

[b] Decommissioned wells but provide historical "pre-cover" groundwater information

Results and discussion

Meteorological conditions

Figure 4 presents the monthly and cumulative PPT between January 2012 and December 2016. The annual cumulative amount of PPT was 1191, 1311, 1322, 1426, and 1442 mm in 2012, 2013, 2014, 2015, and 2016, respectively. The WRP experienced a range of weather conditions, with the highest PPT in the fall and winter periods. Snow accounted for 18, 30, 23, 31, and 26% of PPT each year from 2012 to 2016, respectively.

PE is also shown in Fig. 4, with annual total fluxes equal to 607, 612, 608, 524, and 537 mm between 2012 and 2016, respectively. PPT exceeded PE for the majority of each year, creating a surplus of water that needs to be managed by the cover system through runoff and NP. During dry summer periods, PE and AET would adequately manage PPT through the store-and-release of water in the cover material.

Cover material conditions

Water dynamics

1. Changes in water storage

   Figure 5 presents the total volume of water in the cover material at each SMS between January 2014 and December 2014. The most significant increase in water volumes occurred in spring when PPT and snowmelt were high and AET was low. In the summer, low PPT and increased AET resulted in significant water loss, with the combination of increased PPT and low AET allowing replenishment of stored water in the fall. It is evident that water volumes were lower at SMS-4 during periods of high PPT (i.e., spring and fall) due to higher surface water runoff, while during summer, water volumes were lower on the plateau SMSs due to the southern azimuth and higher evaporation.
2. Hydraulic gradient at the cover–waste rock interface

   In situ matric suction measured at nine depths at each SMS were used to investigate hydraulic gradients throughout the cover and shallow waste rock. Figure 6 presents the hydraulic gradient across the cover–waste rock interface at SMS-3 and SMS-4 between January 2014 and December 2014. SMS-3 and SMS-4 exhibited the largest differences in total water volumes in Fig. 5 and are also included in Fig. 6. Field capacity of the growth medium was estimated to be approximately 125 mm based on the observed water dynamics. The estimated field capacity of the growth medium is indicated by the dashed line. The field capacity refers to the total volume of water in the soil profile after all water has been removed by gravity and therefore gave an indication of the moisture conditions when downward movement of water into the waste material was likely to occur.

The hydraulic gradient was predominantly downward (i.e., positive). During winter, the gradient fluctuates from positive to negative due to pore-water freezing at the interface. At the freezing front, a low pressure condition was established which can

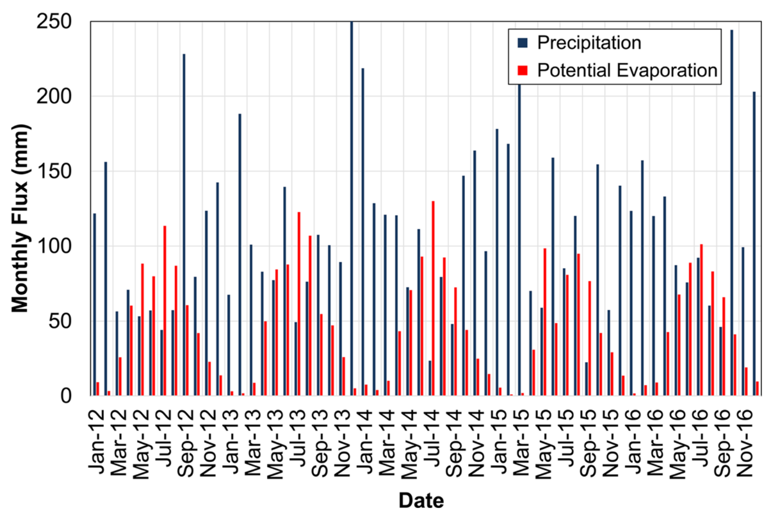

Fig. 4 Monthly precipitation and potential evaporation between January 2012 and December 2016

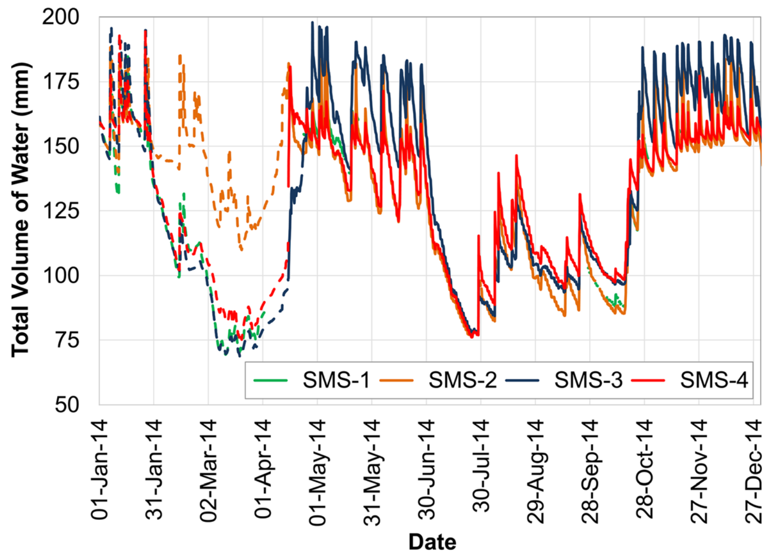

Fig. 5 Total volume of water in the cover at each SMS between January 2014 and December 2014. The TDR sensor detects only unfrozen water, so frozen pore-water conditions are indicated by dashed lines

lead to changes in hydraulic gradient. The hydraulic gradient was similar in the spring and fall when water volumes in the cover profile were high (above or near field capacity) and AET is low. In comparison, the gradient fluctuated to an upward direction in the summer when AET became a greater component of the water balance.

3. Surface runoff

The hourly stage measurements at the weir were used to measure the volume of runoff at the WRP. Using a contributing area of 26,000 m^2 for the cover system, the estimated runoff from the cover system was 418, 454, 534, 535, and 541 mm for each year between 2012 and 2016.

4. Actual evapotranspiration

Following rainfall, when surface conditions are wet, the AET/PE ratio was at its highest. This ratio then continuously decreased given that negative pore-water pressure (suction) in the soil profile increased as the surface desiccates. In 2014, AET was estimated at 414 mm, which is 68% of PE.

Water influx

Table 3 presents the flux of each component and their ratio to PPT (%). Using 2014 as an example, total PPT was 1195 mm with 2 mm stored in snow over the winter

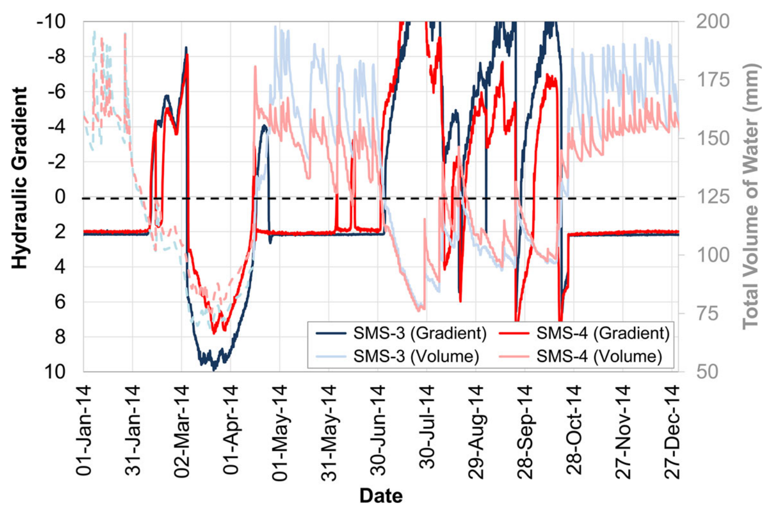

Fig. 6 Hydraulic gradient measured across the cover–waste rock interface at each SMS between January 2014 and December 2014

Table 3 Annual water and oxygen flux components between 2012 and 2016

Component	2012		2013		2014		2015		2016		Mean	
Water	mm	%[a]	mm	%	mm	%	mm	%	mm	%	mm	%
PPT	1191	–	1311	–	1322	–	1426	–	1442	–	1338	–
R	418	35	454	35	534	45	535	37	541	38	496	37
AET	408	34	416	32	414	34	356	25	365	25	392	30
ΔWS	−13	0	3	0	−5	0	8	1	19	1	2	0
ΔSS	3	0	127	9	2	0	128	9	111	8	74	5
NP	375	31	311	24	377	31	399	28	406	28	374	28
Oxygen	mol/m^2		mol/m^2		mol/m^2		mol/m^2		mol/m^2		mol/m^2	
Diffusion	46.33		62.47		78.39		20.48		40.04		49.54	
Dissolved	0.044		0.036		0.044		0.046		0.047		0.043	
Total	46.37		62.51		78.44		20.48		40.04		49.58	

[a] Each water balance component is also indicated as a percentage of precipitation (% PPT)

months. Of PPT, 534 mm was estimated to leave the WRP as runoff while another 414 mm was estimated to leave the WRP as AET. A negligible amount of water was stored in the cover system, and a NP of 377 mm into the waste rock was estimated using Eq. (2). Figure 7 illustrates the cumulative flux for each component in 2014. As expected, the majority of NP occurred during winter periods where PPT was high and AET was low.

As shown in Table 3, the mean annual NP rate between 2012 and 2016 was 374 mm (mean NP/PPT = 28%), demonstrating that the cover did not significantly limit water influx to the waste rock. As expected, it is higher than multilayer soil covers that are able to maintain a high degree of saturation throughout the year (e.g., O'Kane et al. 1998; Adu-Wusu et al. 2007). Nevertheless, it is similar to previous NP rates through single-layer soil covers (e.g., Barber et al. 2015) and does provide a reduction from pre-cover NP estimates: using the NP/PPT ratio of 34% demonstrated on similar waste rock/fill material (King et al. 2003), the pre-cover NP was estimated at 434 mm. Since drain-down is expected to have already occurred, and NP has not changed significantly between 2012 and 2016, the WRP is assumed to be at steady-state water content. As a result,

Fig. 7 Cumulative flux for each component of the Lingan WRP water balance in 2014

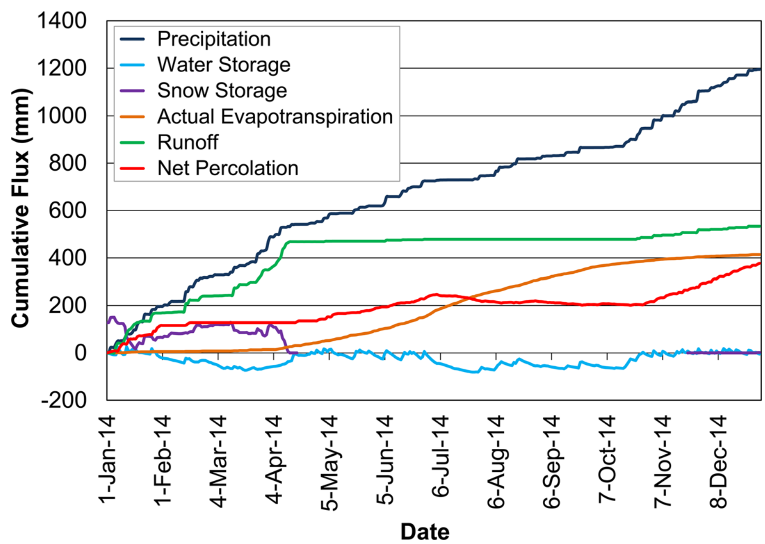

the seepage rate through the waste rock and into underlying groundwater should be equal to NP.

NP is expected to continue to vary in the long-term as cover system vegetation evolves and climatic conditions change. It is acknowledged that extensive conclusions on cover performance cannot be inferred from this initial monitoring period alone, and it is only when examining NP over the long term and in the overall context of normal climate variability that trends in performance can be determined. Current work involves the calibration of the soil-atmosphere model VADOSE/W (Krahn 2004) to both plateau and slope field conditions at the WRP (e.g., SMS-2, SMS-4). The fully calibrated model, incorporating climate variability, will then be used to evaluate and predict long-term cover system conditions (e.g., Adu-Wusu et al. 2007).

Oxygen influx

Figure 8 presents the mean O_2 and CO_2 concentrations measured at depths of 0.48, 0.55, and 1.2 m at the four SMSs between January 2012 and December 2014. The concentrations in 2015 and 2016 are not included due to concerns over data reliability.

It is evident that O_2 concentrations generally follow the same trend at all depths, with lower O_2 below the cover–waste rock interface (red circles and gray diamonds in Fig. 8). Depleted O_2 and elevated CO_2 occur during summer periods which may be related to the oxidation of organic material in the cover material or carbonaceous material in the shallow waste rock. Some of the high concentrations observed below the cover during fall and winter periods were not likely representative; relatively high in situ moisture conditions during fall could have reduced flow volumes in the sampling tubes and led to atmospheric conditions entering the system, while these relatively shallow sampling tubes could have frozen during winter.

Figure 9 plots the cumulative diffusive and dissolved O_2 flux in 2014. Diffusive flux was the dominant mechanism and showed the most significant increase during July and August where moisture content and the corresponding diffusivity coefficient were the lowest. Although diffusive flux also showed an increase during winter, this was during freezing periods where measured moisture contents were likely inaccurate. Dissolved flux generally followed the same trend as NP in Fig. 7, with highest flux during periods of high NP (i.e., spring and fall). The total O_2 flux in 2014 was 78.44 mol/m^2.

The annual cumulative flux for each O_2 component is shown in Table 3, with the total flux rates ranging from 20.48 to 78.44 mol/m^2. These high flux rates indicate that the cover system did not effectively limit O_2 ingress. In contrast, Aubertin et al. (2000) demonstrated that GCL covers can limit O_2 flux to approximately 4 mol/m^2. Nevertheless, significantly limiting O_2 ingress in a store-and-release cover is typically not a performance criterion, even in semi-arid and arid climates.

Internal pile conditions

Pore-gas concentrations

Mean O_2 and CO_2 concentrations measured at each IMS between January 2012 and December 2016 at four depths within the waste rock are presented in Fig. 10.

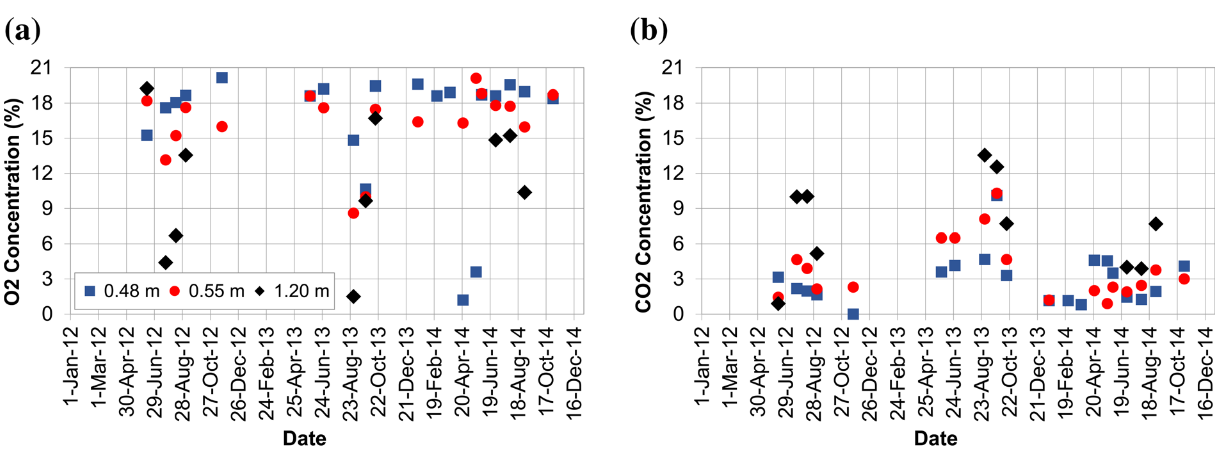

Fig. 8 Mean **a** O_2 and **b** CO_2 concentrations measured at the four SMSs between January 2012 and December 2014

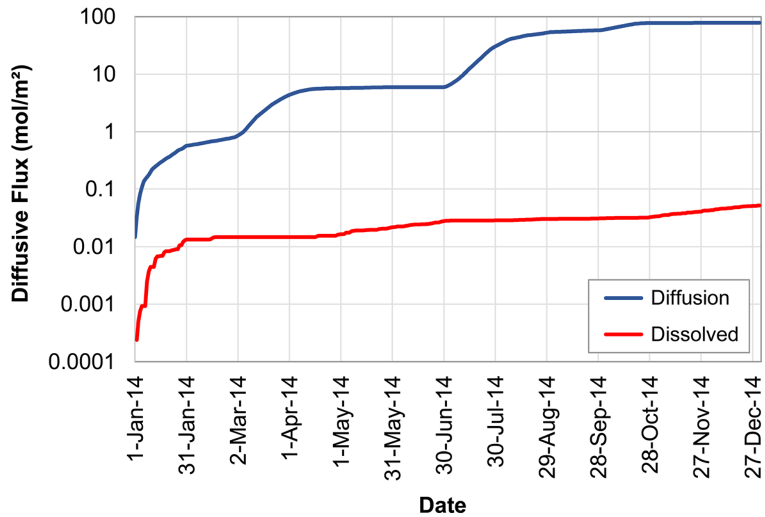

Fig. 9 Cumulative O_2 flux through the cover material between January 2014 and December 2014

Throughout the monitoring period, O_2 and CO_2 concentrations fluctuated between a minimum 0% and maximum 17%. A pattern did exist, particularly with the two deepest measurements (i.e., 10.08 and 12.65 m), with O_2 generally decreasing during the summer with a corresponding increase in CO_2. The variation in pore-gas is indicative of the oxidation process expected in an acid generating WRP, with the oxidation of sulfide minerals resulting in the consumption of O_2 and production of CO_2 when the generated acid reacts with carbonates in the system.

Waste rock acidity

Table 4 provides a summary of ABA results on the eight IMS waste rock samples. Due to the measured low paste pH values, negative ANP values, and low ANP/AGP ratios (< 1), the waste rock was classified as acid generating. These 2011 results were similar to the more comprehensive ABA testing conducted in 2008 on 26 waste rock samples. The mean acid generation potential (AGP) of 11.50 kg $CaCO_3$/t indicated a potential acidity volume of 7432 t. Based on the mean 0.34 wt% sulfate-sulfur content, 10.71 kg $CaCO_3$/t was present as stored acidity, indicating a total volume of 6922 t.

Pyrite oxidation rate

The total O_2 flux in Table 3 was converted to an acidity load on the basis of H_2SO_4 equivalent (mol/m^2/year). Using Eq. (5), 2 mol of acid is generated per 3.75 mol of

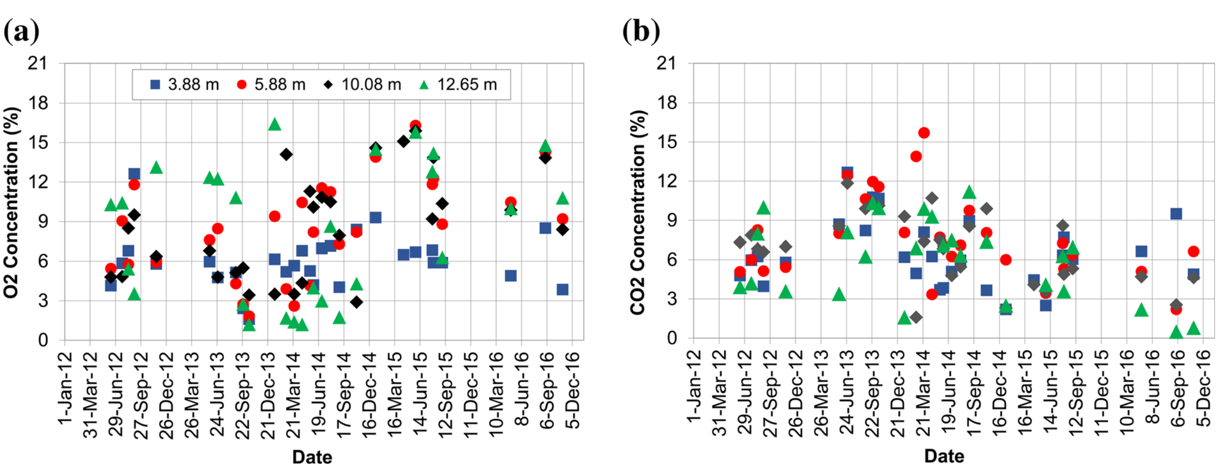

Fig. 10 Mean **a** O_2 and **b** CO_2 concentrations measured at the four IMSs between January 2012 and December 2016

Table 4 Summary of ABA tests ($N = 8$), including paste pH, total sulfur, ANP, AGP, and NNP

Sample	Paste pH –	Total S wt%	Sulfide wt%	Sulfate wt%	ANP kg $CaCO_3$/t	AGP kg $CaCO_3$/t	NNP kg $CaCO_3$/t
Mean	4.75	0.71	0.37	0.34	− 0.38	11.50	− 11.88
Min-max	3.2–7.2	0.17–0.99	0.10–0.60	0.07–0.51	− 8.66 to 6.95	3.06–18.63	− 23.97 to 3.89
Std dev	1.63	0.28	0.16	0.15	6.49	5.10	9.45

O_2. The 2012–2016 mean O_2 flux of 49.58 mol O_2/m^2/year generated 26.44 mol H_2SO_4/m^2/year. Using this acidity rate, the total extrapolated catchment acidity load over the area of the cover system was 216.83 t of acidity per year (as $CaCO_3$).

Impacts to environmental receptors

Groundwater flow

To develop the representative piezometric surface and flow direction within the WRP area, the mean IMS groundwater levels measured every September between 2012 and 2016 were combined with the historical site groundwater levels measured in September 2008. The resulting groundwater flow regime is illustrated in Fig. 11. It clearly demonstrates that groundwater flows from east to west beneath the WRP and then downgradient towards the northwest. It is also evident that upgradient groundwater first interacts with IMS-1 and IMS-2 along its flow path, while IMS-3 and IMS-4 can be considered further downgradient.

Groundwater quality

Figure 12 plots the evolution of key parameters that characterize AMD (i.e., sulfate, pH, alkalinity, dissolved concentrations of iron, aluminum, and manganese) between June 2012 and December 2016. Sulfate, which is considered as the most representative AMD indicator due to its high persistence in groundwater, is presented in Fig. 12a. While concentrations at IMS-1 (blue squares) and IMS-2 (red circles) do not demonstrate a consistent reduction between 2012 and 2016, IMS-3 (black diamonds) and IMS-4 (green triangles) show a general decrease in sulfate concentration. These trends are also evident upon comparison of IMS-1 and IMS-2 to background well MW-11 (no significant change) and IMS-3 and IMS-4 to background well MW-02 (gradual reduction over time). Figure 12a also indicates a coarse annual pattern at each IMS, particularly IMS-3 and IMS-4, with sulfate showing an increase every July and August which corresponds to times of low O_2 and high CO_2 (i.e., indications of increased AMD generation) measured near the base of the WRP in Fig. 10.

The pH and dissolved metal concentrations in Fig. 12b–e follow a similar trend to sulfate concentrations between 2012 and 2016, with no significant change at IMS-1 and IMS-2 but a gradual improvement at IMS-3 and IMS-4. However, comparisons to pre-cover quality at MW-11 and MW-02 demonstrated that all IMS locations have improved since December 2008. Dissolved metal concentrations also show the trend of increasing concentrations during July and August each year. Figure 12f demonstrates an increase in alkalinity at all IMSs. Toe seepage water quality measured between April 2015 and December 2016 was also plotted for each parameter in Fig. 12 (black x's). As expected, water quality at the seep was similar to that at each IMS, particularly IMS-4, which was expected as they are both located in similar downgradient regions of the pile.

Health Canada drinking water guideline concentrations for each parameter are shown by black dashed lines in Fig. 12. It is evident that all parameters generally fluctuated around or within the guidelines, except for iron and manganese.

Surface water quality

The key parameters for groundwater were also analyzed for surface water and are plotted in Fig. 13. Water quality steadily improved at the downstream SW-01 sampling point following cover system installation. In Fig. 13a, sulfate concentrations upstream of the WRP (SW-05) remained the same, while downstream sulfate concentrations (SW-01) were improving, particularly since 2012. At SW-01, dissolved metals were also steadily decreasing, while pH and alkalinity were increasing. Canadian Council of Ministers of the

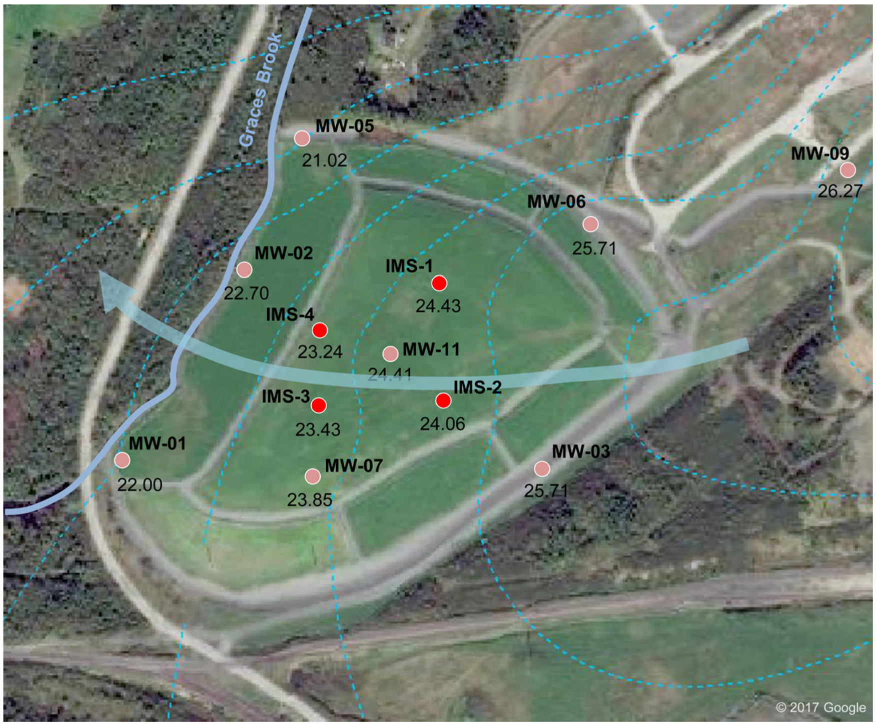

Fig. 11 Groundwater piezometric surface and flow direction beneath the Lingan WRP

Environment (CCME) aquatic water quality guideline concentrations for each parameter (where available) are shown by black dashed lines in Fig. 13 and indicate that all parameters consistently lie within the guidelines.

In addition to improvements in water quality, visual observations along Graces Brook demonstrate that the cover system is facilitating the recovery of aquatic and vegetative life. Although the cover system did not significantly reduce water influx into the WRP, it has eliminated the contaminated surface water runoff previously entering Graces Brook. This could be considered the largest direct impact that the cover system provided at the site.

Estimate of WRP acidity depletion

The mean calculated acidity at IMS-1 to IMS-4 between 2012 and 2016 was 23.85, 9.01, 9.56, and 71.17 mg/L, respectively, to provide a WRP average of 28.40 mg/L. This acidity was combined with the mean NP (equal to basal seepage) of 0.97 L/s (374 mm/year) to provide a mean acidity loading from the WRP of 0.87 t/yr.

The total potential acidity load based on O_2 flux was 216.83 t/yr. which indicates a high ongoing oxidation rate for sulfide minerals within the WRP. Since the total potential acidity was 7432 t, 2.9% of this potential acidity will oxidize each year. Consequently, it will take approximately 34 years to fully deplete the potential acidity.

Since this oxidation rate of 216.83 t is much larger than the acidity seepage rate of 0.82 t, the stored acidity in the pile will actually increase by 215.79 t each year for the 34 years to complete oxidation. At that time, the original stored acidity of 6922 t will have increased to 14,324 t. Assuming a constant seepage rate of 0.87 t/year, it will take an estimated 16,500 years for full WRP acidity depletion. It is acknowledged that this is an extremely simplistic estimate and that numerical modeling is required to obtain accurate predictions of long-term WRP acidity depletion.

Landform stability and vegetation

Numerous site surveys indicated that there was no significant visible erosion of the landform and the landform was determined to be stable (geomorphically and geotechnically). Vegetation on the WRP is thriving, as shown in the site photos in Figs. 1 and 3, which further enhances erosion resistance, improves site aesthetics, and creates wildlife habitat. Furthermore, a more mature

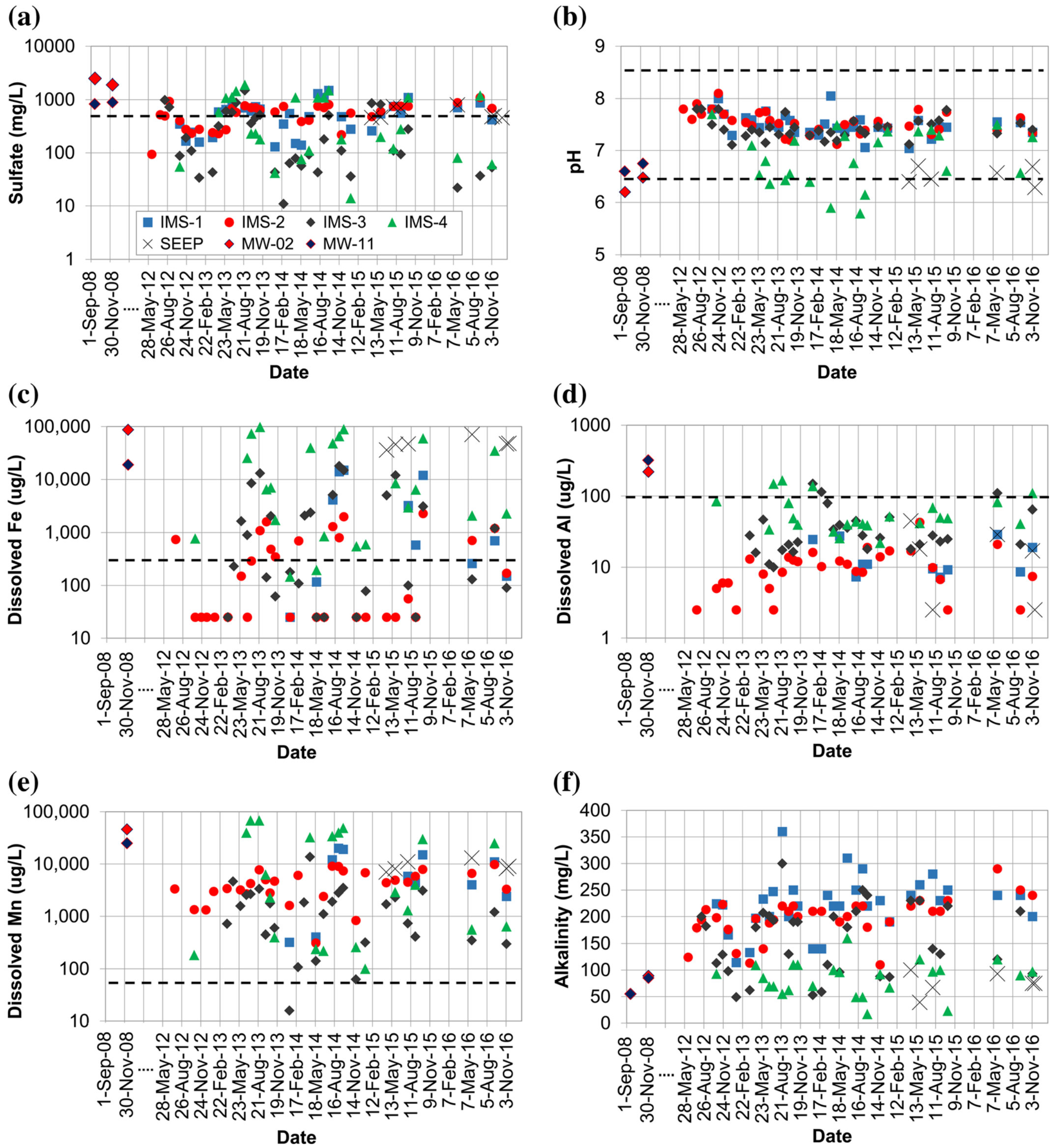

Fig. 12 Evolution of **a** sulfate, **b** pH, **c** dissolved iron, **d** dissolved aluminum, **e** dissolved manganese, and **f** alkalinity in groundwater at each IMS between September 2008 and December 2016. Toe seepage and pre-cover water quality (MW-02 and MW-11) are also plotted, while Health Canada Drinking Water Guidelines are shown by the black dashed line

vegetation cover contributes to lower NP and seepage volumes through increased interception and transpiration rates (Barber et al. 2015).

Limitations

In this study, a number of simplifying assumptions were used. WRPs are typically complex and heterogeneous and the assumption of homogeneity simplifies water flow/distribution and geochemical characterization of the waste rock. For example, analysis of spatial and temporal conditions across the WRP are based on parameters collected from four sampling points (i.e., SMSs and IMSs). However, it is common practice in any field study to rely on, and interpolate between, sparsely distributed sample locations. Furthermore, the four sampling points were distributed to be as representative as possible of site conditions, with three sampling points located on the plateau and one sampling point located on the slope. This spatial variation was evident in the presented results.

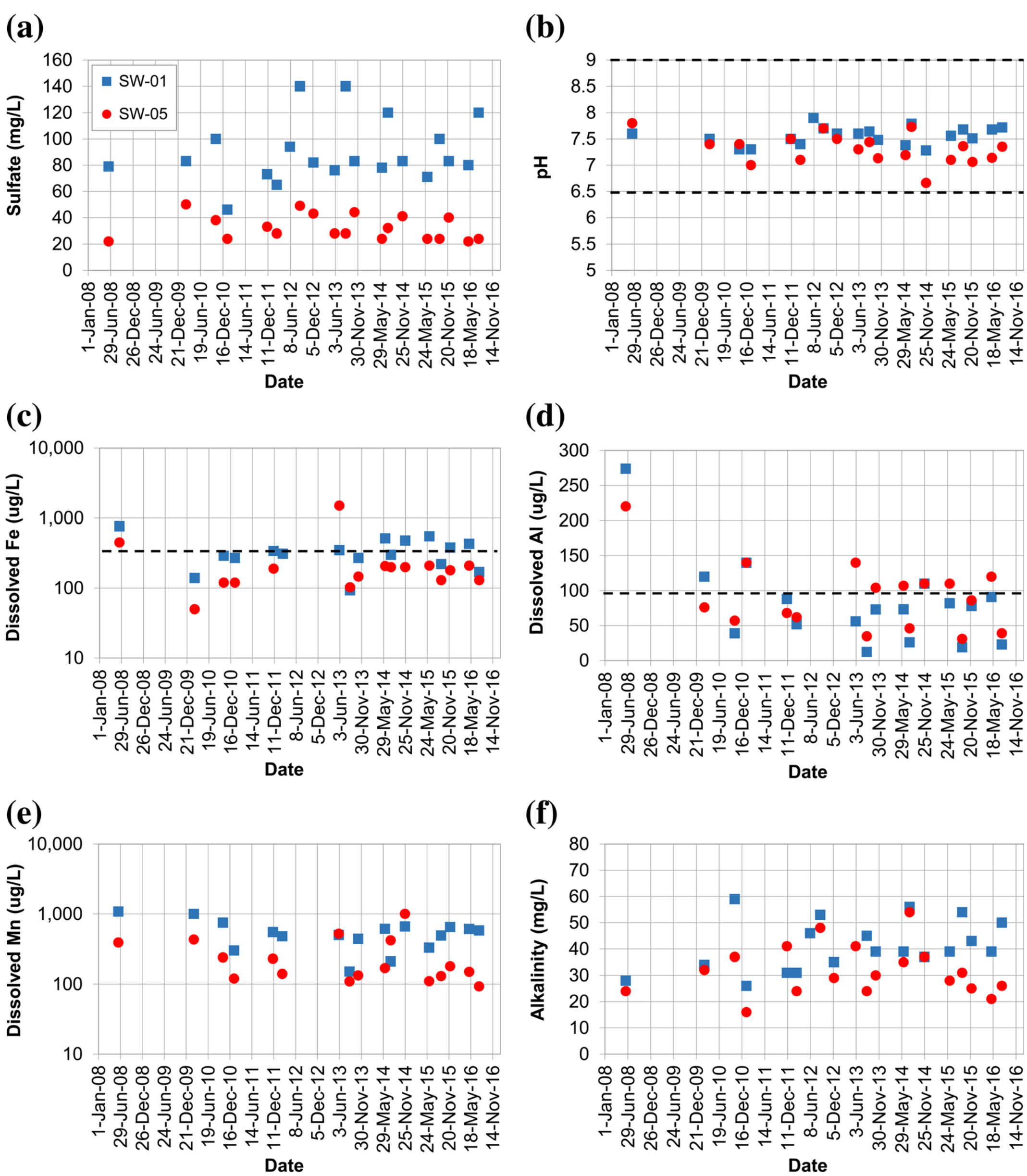

Fig. 13 Evolution of **a** sulfate, **b** pH, **c** dissolved iron, **d** dissolved aluminum, **e** dissolved manganese, and **f** alkalinity in Graces Brook at upstream (SW-05) and downstream (SW-01) locations between January 2008 and December 2016

Mean values from eight ABA waste rock samples were used to estimate potential and stored acidity volumes in the WRP, which were subsequently used to estimate the depletion rate of acidity in the WRP. It is acknowledged that this estimate, using mean values of water acidity and seepage rates from the WRP and assuming they remain constant in the long-term, is coarse and highly simplistic.

It was not possible to collect pore-water samples within the waste rock so samples taken from the underlying groundwater were used to represent WRP seepage water quality. These samples were likely already diluted with upgradient groundwater, thereby underestimating actual AMD concentrations and loading. However, AMD loading was represented by calculated acidity in Eq. (6) which does not account for the neutralization capacity of alkaline minerals in the waste rock, such as carbonates and silicates. This overestimation of AMD should offset some of the underestimated AMD due to the aforementioned groundwater dilution.

The sulfide oxidation rate was assumed to be equal to the O_2 influx to the waste rock. The effects of pre-oxidation (e.g., Pabst et al. 2017) were not considered, along with thermal advection and convection. Laboratory tests with humidity cells and leaching columns on the extracted waste rock samples (i.e., already used for ABA tests) can be used to assess various kinetic aspects such as the velocity of sulfide oxidation and metal leaching rates (e.g., Plante et al. 2014). This kinetic data will help to more accurately access the generation and release of AMD.

While this study provides a direct assessment of cover performance and AMD evolution over a relatively short time period, numerical modeling is required to evaluate long-term performance. A variably saturated flow and contaminant transport model is currently being developed in FEFLOW (Diersch 2014) and validated to the 5-year field dataset. It will incorporate long-term climatic variations and examine long-term spatial and temporal evolution of cover performance, AMD loading, and impacts to the receiving environment. In the future, this model can be integrated with the PHREEQC geochemical reaction model (Charlton and Parkhurst 2011) to include kinetic and multiphase transfer processes.

Conclusions

The performance of a single-layer moisture store-and-release cover system installed at a WRP in a humid climate was directly assessed. The WRP at the former Lingan Mine Colliery in Nova Scotia, Canada, was reclaimed with a store-and-release cover in 2011, followed by 5 years of comprehensive field monitoring of meteorological, geological, geochemical, and hydrogeological conditions.

PPT exceeded AET for large periods of the year, creating a surplus of water that needed to be managed by the cover system. While the store-and-release process limited water infiltration during dry summer periods, it was not effective during periods in the spring and fall (snowmelt and rainfall events) with high water infiltration rates correlating to periods of high water storage and downward hydraulic gradients in the cover. Although the mean annual infiltration reduced from 34 to 28% PPT, the cover is not a highly effective barrier to water infiltration in humid climates. However, performance criteria at some WRPs, particularly those with low AMD concentrations, may just require the preservation of existing infiltration and AMD loading rates following site closure.

The cover system was highly effective in meeting other performance criteria. The placement of the cover over the previously exposed waste rock ensured only clean surface water runoff to the surface water receptor, with AMD loading to the receptor now provided by a single toe seep and groundwater discharge. This led to significant improvements in surface water quality, which was also indicated by direct observations of recovery in aquatic life and vegetation. The cover also provided a stable (geomorphically and geotechnically) landform and established a sustainable and thriving vegetative canopy. Overall, the cover provided a measurable positive effect on the environment compared to pre-cover impact.

The performance of the cover system will evolve over time in response to climatic conditions and site-specific physical, chemical, and biological processes. A variably saturated flow and contaminant transport model is currently being developed in FEFLOW to predict long-term cover performance under long-term average and extreme climatic conditions. In addition, the soil-plant-atmosphere model VADOSE/W will be calibrated to the collected field data and then used to evaluate long-term water and oxygen flux rates through the cover. The integration of these predictive models with ongoing field monitoring will provide a rigorous assessment of long-term cover system performance.

Acknowledgements This work was conducted under the CAPs Monitoring Project and funded by Enterprise Cape Breton Corporation (ECBC) which was later dissolved into Public Works and Government Services Canada (PWGSC). The authors wish to thank the anonymous reviewers for their helpful comments towards the improvement of this paper. Special thanks are given to Joseph MacPhee and Joseph Shea (PWGSC) and Devin MacAskill (Cape Breton Regional Municipality, CBRM) for their support during this study. The authors would also like to acknowledge Greg Meiers (O'Kane Consultants) for sharing his expertise, along with David Mayich, Fred Baechler (exp Consultants), and Jamie Tunnicliff (Stantec Consulting Ltd.).

References

Adu-Wusu, C., & Yanful, E. K. (2006). Performance of engineered test covers on acid-generating waste rock at Whistle mine, Ontario. *Canadian Geotechnical Journal, 43*(1), 1–18. https://doi.org/10.1139/t05-088.

Adu-Wusu, C., Yanful, E. K., Lanteigne, L., & O'Kane, M. (2007). Prediction of the water balance of two soil cover systems. *Geotechnical and Geological Engineering, 25*(2), 215–237. https://doi.org/10.1007/s10706-006-9106-3.

Akcil, A., & Koldas, K. S. (2006). Acid mine drainage (AMD): causes, treatment and case studies. *Journal of Cleaner Production, 14*, 1139–1146. https://doi.org/10.1016/j.jclepro.2004.09.006.

Albright, W. H., Benson, C. H., Gee, G. W., Abichou, T., Tyler, S. W., & Rock, S. A. (2006). Field performance of three compacted clay landfill covers. *Vadoze Zone Journal, 5*(4), 1157–1171. https://doi.org/10.2136/vzj2005.0134.

Amos, R. T., Blowes, D. W., Bailey, B. L., Sego, D. C., Smith, L., & Ritchie, A. I. M. (2015). Waste-rock hydrogeology and geochemistry. *Applied Geochemistry, 57*, 140–156. https://doi.org/10.1016/j.apgeochem.2014.06.020.

Aubertin, M., Aachib, M., & Authier, K. (2000). Evaluation of diffusive gas flux through covers with a GCL. *Geotextiles and Geomembranes, 18*(2–4), 215–233. https://doi.org/10.1016/S0266-1144(99)00028-X.

Ayres, B., Dirom, G., Christensen, D., Januszewski, S., O'Kane, M. (2003). Performance of cover system field trials for waste rock at Myra Falls Operations. In: T. Farrell, & G. Taylor (Eds.), Proceedings of the 6th International Conference on Acid Rock Drainage (ICARD), 12–18 July 2003, Cairns, QLD, Australia. ISBN: 1875776982.

Barber, L. A., Ayres, B. K., Schmid, B. (2015) Performance evaluation of reclamation soil covers at Cluff Lake mine in northern Saskatchewan. In: A. B. Fourie, M. Tibbett, L. Sawatsky, & D. van Zyl (Eds.), Mine Closure 2015: Proceedings of the Tenth International Conference on Mine Closure, 1–3 June 2015, Vancouver, BC, Canada. Australian Centre for Geomechanics, Perth. ISBN 9780991790593.

Benson, C. H., Thorstad, P. A., Jo, H., & Rock, S. A. (2007). Hydraulic performance of geosynthetic clay liners in a landfill final cover. *Journal of Geotechnical and Geoenvironmental Engineering, 133*(7), 814–827. https://doi.org/10.1061/(ASCE)1090-0241(2007)133:7(814).

Blowes, D. W., Ptacek, C. J., Jambor, J. L., Weisener, C. G., Paktunc, D., Gould, W. D., & Johnson, D. B. (2014). 11.5—The geochemistry of acid mine drainage. In: H. D. Holland, & K. K. Turekian (Eds.), *Treatise on geochemistry*, 2nd edn. (pp. 131–190). Oxford: Elsevier. https://doi.org/10.1016/B978-0-08-095975-7.00905-0.

Bonstrom, K., Allen, G., O'Kane, M., Christensen, D. (2012). Evolution of cover system design and waste rock management at a mine in the Pilbara region of Western Australia. In: A. B. Fourie, & M. Tibbett (Eds.), Mine Closure 2012: Proceedings of the Seventh International Conference on Mine Closure, 25–27 September 2012, Brisbane, Australia. Australian Centre for Geomechanics, Perth. ISBN 9780987093707.

Charlton, S. R., & Parkhurst, D. L. (2011). Modules based on the geochemical model PHREEQC for use in scripting and programming languages. *Computers and Geosciences, 37*(*10*), 1653–1663. https://doi.org/10.1016/j.cageo.2011.02.005.

Diersch, H. J. G. (2014). *FEFLOW: Finite element modeling of flow, mass and heat transport in porous and fractured media* (p. 996). Berlin: Springer-Verlag. https://doi.org/10.1007/978-3-642-38739-5.

INAP (The International Network for Acid Prevention). (2014). Global acid rock drainage guide. http://gardguide.com/images/5/5f/TheGlobalAcidRockDrainageGuide.pdf Accessed 22 June 2017.

Johnson, D. B., & Hallberg, K. B. (2005). Acid mine drainage remediation options: a review. *Science of the Total Environment, 338*, 3–14. https://doi.org/10.1016/j.scitotenv.2004.09.002.

Kefeni, K. K., Msagati, T. A. M., & Mamba, B. B. (2017). Acid mine drainage: prevention, treatment options, and resource recovery: a review. *Journal of Cleaner Production, 151*, 475–493. https://doi.org/10.1016/j.jclepro.2017.03.082.

Kim, H., & Benson, C. H. (2004). Contributions of advective and diffusive oxygen transport through multilayer composite caps over mine waste. *Journal of Contaminant Hydrology, 71*(1–4), 193–218. https://doi.org/10.1016/j.jconhyd.2003.10.001.

King, M., Check, G., Carey, G., Abbey, D., Baechler, F. (2003). Groundwater and contaminant transport modelling at the Sydney Tar Ponds. In: Canadian Geotechnical Society. Proceedings of 56th Annual Canadian Geotechnical Conference and 4th Joint IAH-CNC/CGS Groundwater Specialty Conference, September 29–October 1, 2003, Winnipeg, Manitoba, Canada.

Kirby, C. S., & Cravotta III, C. A. (2005). Net alkalinity and net acidity 1: theoretical considerations. *Applied Geochemistry, 20*, 1920–1940. https://doi.org/10.1016/j.apgeochem.2005.07.002.

Krahn, J. (2004). *Vadose zone modeling with VADOSE/W: an engineering methodology* (1st ed.). Calgary: GEO-SLOPE International Ltd.

Meer, S. R., & Benson, C. H. (2007). Hydraulic conductivity of geosynthetic clay liners exhumed from landfill final covers. *Journal of Geotechnical and Geoenvironmental Engineering, 133*(5), 550–563. https://doi.org/10.1061/(ASCE)1090-0241(2007)133:5(550).

MEND (Mine Environment Neutral Drainage). (2004). Design, construction and performance monitoring of cover systems for waste rock and tailings: volume 1—summary. Canadian Mine Environment Neutral Drainage Program, Project 2.21.4a, July 2004. http://mend-nedem.org/wp-content/uploads/2.21.4a-Cover-Design-Manual.pdf. Accessed 15 May 2017.

Nordstrom, D. K., Blowes, D. W., & Ptacek, C. J. (2015). Hydrogeochemistry and microbiology or mine drainage: an update. *Applied Geochemistry, 57*, 3–16. https://doi.org/10.1016/j.apgeochem.2015.02.008.

O'Kane, M., & Ayres, B. (2012). Cover systems that utilise the moisture store-and-release concept—do they work and how can we improve their design and performance? In: A. B. Fourie, & M. Tibbett (Eds.), Mine Closure 2012: Proceedings of the Seventh International Conference on Mine Closure, 25–27 September 2012, Brisbane, Australia. Australian Centre for Geomechanics, Perth. ISBN 9780987093707.

O'Kane, M., Wilson, G. W., & Barbour, S. L. (1998). Instrumentation and monitoring of an engineered soil cover system for mine waste rock. *Canadian Geotechnical Journal, 35*(5), 828–846. https://doi.org/10.1139/t98-051.

Pabst, T., Molson, J., Aubertin, M., & Bussière, B. (2017). Reactive transport modelling of the hydro-geochemical behaviour of partially oxidized acid-generating mine tailings with a monolayer cover. *Applied Geochemistry, 78*, 219–233.

Parbhakar-Fox, A., & Lottermoser, B. G. (2015). A critical review of acid rock drainage prediction methods and practices.

Minerals Engineering, 82, 107–124. https://doi.org/10.1016/j.mineng.2015.03.015.

Park, D., Park, B., Mendinsky, J. J., Paksuchon, B., Suhataikul, R., Dempsey, B. A., & Cho, Y. (2015). Evaluation of acidity estimation methods for mine drainage, Pennsylvania, USA. *Environmental Monitoring and Assessment, 187*, 4095. https://doi.org/10.1007/s10661-014-4095-9.

Penman, H. L. (1948). Natural evaporation from open water, bare soil and grass. *Proceedings of the Royal Society of London. Series A, 193*, 120–145. https://doi.org/10.1098/rspa.1948.0037.

Plante, B., Bussière, B., & Benzaazoua, M. (2014). Lab to field scale effects on contaminated neutral drainage prediction from the Tio mine waste rocks. *Journal of Geochemical Exploration, 137*, 37–47. https://doi.org/10.1016/j.gexplo.2013.11.004.

Power, C., Ramasamy, M., MacAskill, D., Shea, J., MacPhee, J., Mayich, D., Baechler, F., & Mkandawire, M. (2017). Five-year performance monitoring of a high-density polyethylene (HDPE) cover system at a reclaimed mine waste rock pile in the Sydney Coalfield (Nova Scotia, Canada). *Environmental Science and Pollution Research, 24*(34), 26744–26762. https://doi.org/10.1007/s11356-017-0288-4.

Power, C., Tsourlos, P., Ramasamy, M., Nivorlis, A., & Mkandawire, M. (2018). Combined DC resistivity and induced polarization (DC-IP) for mapping the internal composition of a mine waste rock pile in Nova Scotia, Canada. *Journal of Applied Geophysics, 150* 40–51. https://doi.org/10.1016/j.jappgeo.2018.01.009.

Salinas Villafane, O. R., Igarashi, T., Harada, S., Kurosawa, M., & Takase, T. (2012). Effect of different soil layers on porewater to remediate acidic surface environment at a close mine site. *Environmental Monitoring and Assessment, 184*(12), 7665–7675. https://doi.org/10.1007/s10661-012-2526-z.

Scanlon, B. R., Reedy, R. C., Keese, K. E., & Dwyer, S. F. (2005). Evaluation of evapotranspirative covers for waste containment in arid and semi-arid regions in the southwestern USA. *Vadose Zone Journal, 4*(1), 55–71. https://doi.org/10.2113/4.1.55.

Sracek, O., Gzyl, G., Frolik, A., Kubica, J., Bzowski, Z., Gwozdziewicz, M., & Kura, K. (2010). Evaluation of the impacts of mine drainage from a coal waste pile on the surrounding environment at Smolnica, southern Poland. *Environmental Monitoring and Assessment, 165*(1–4), 233–254. https://doi.org/10.1007/s10661-009-0941-6.

Watzlaf, G. R., Schroeder, K. T., Kleinmann, R. L. P., Kairies, C. L., Nairn, R. W. (2004). The passive treatment of coal mine drainage. U.S. Department of Energy, DOE/NETL-2004/1202.

Yucel, D. S., & Baba, A. (2016). Prediction of acid mine drainage generation potential of various lithologies using static tests: Etili coal mine (NW Turkey) as a case study. *Environmental Monitoring and Assessment, 188*(8), 473. https://doi.org/10.1007/s10661-016-5462-5.